Testing the very-short-baseline neutrino anomalies at the solar sector

Antonio Palazzo

Cluster of Excellence, Origin and Structure of the Universe, Technische Universität München, Boltzmannnstraße 2, D-85748, Garching, Germany

(Received 24 May 2011; published 23 June 2011)

Motivated by the accumulating hints of new sterile neutrino species at the eV scale, we explore the consequences of such an hypothesis on the solar sector phenomenology. After introducing the theoretical formalism needed to describe the Mikheyev-Smirnov-Wolfenstein conversion of solar neutrinos in the presence of one (or more) sterile neutrino state(s) located "far" from the (ν_1, ν_2) "doublet", we perform a quantitative analysis of the available experimental results, focusing on the electron neutrino mixing. We find that the present data posses a sensitivity to the amplitude of the lepton mixing matrix element U_{e4}—encoding the admixture of the electron neutrino with a new mass eigenstate—which is comparable to that achieved on the standard matrix element U_{e3}. In addition, and more importantly, our analysis evidences that, in a 4-flavor framework, the current preference for $|U_{e3}| \neq 0$ is indistinguishable from that for $|U_{e4}| \neq 0$, having both a similar statistical significance (which is $\sim 1.3\sigma$ adopting the old reactor fluxes determinations, and $\sim 1.8\sigma$ using their new estimates.) We also point out that, differently from the standard 3-flavor case, in a $3+1$ scheme the Dirac CP-violating phases cannot be eliminated from the description of solar neutrino conversions.

DOI: 10.1103/PhysRevD.83.113013 PACS numbers: 14.60.Pq, 14.60.St

I. INTRODUCTION

The interest around the possible manifestation of novel neutrino properties in very short baseline (VSBL) setups has been recently reawakened by the emergence of new (and the reappraisal of old) inconsistencies. Improved calculations of the reactor antineutrino spectra [1] suggest fluxes which are $\sim 3\%$ higher than previous estimates [2–5] and have raised the so-called antineutrino anomaly [6], consisting in a deficit of (almost) all the reactor measurements performed at distances $L \lesssim 100$ m. An apparently unrelated deficit had been already evidenced in the calibration measurements conducted at the solar neutrino experiments GALLEX and SAGE [7,8], employing radioactive sources placed inside the detectors. Such two discrepancies join those already recorded at the VSBL accelerator experiments [9–11], adding further confusion to an already intricate "VSBL neutrino puzzle".

While some of the (old and new) anomalies may be imputable to theoretical and/or experimental inaccuracies, the possibility exists that they may represent a manifestation of new physics. From this perspective, they seem to point towards a phenomenon of (dis-)appearance of the electron neutrinos, possibly mediated by oscillations into new sterile specie(s) [6,8]. Such an hypothesis finds support in the lesser degree of tension—although still a considerable one—now existing between the (weakened) VSBL reactor limits and the (unchanged) VSBL accelerator constraints, within all schemes endowed with additional sterile species [12,13]. Notably, an independent hint in the same direction arises from the latest cosmological data analyses [14], which favor a significant extra relativistic energy content, although pointing towards masses of the new presumptive light particles [14,15], which are at the borderline of those (larger) suggested for the sterile neutrinos by the oscillation data.[1] Such a trend is partially corroborated by the latest constraints coming from primordial nucleosynthesis [18,19], which can easily accommodate one, but hardly two additional sterile species.

The putative sterile neutrinos must be introduced without spoiling the basic success of the standard 3-flavor paradigm. This can be achieved in the so-called $3+s$ schemes, where the s new mass eigenstates are assumed to be separated from the three standard ones by large splittings,[2] giving rise to the hierarchal pattern[3] $|m_2^2 - m_1^2| \ll |m_3^2 - m_1^2| \ll |m_k^2 - m_1^2| (k = 4, \ldots, 3+s)$, which ensures that the fast oscillations induced by the new mass eigenstates are completely averaged in all settings sensitive to the Δm_{12}^2-driven (solar) and Δm_{13}^2-driven (atmospheric) transitions, leaving unmodified the two well-established oscillation frequencies. With the additional assumption of a small admixture of the active flavors

[1]It must be stressed that the degeneracy between the neutrino masses and the dark energy equation of state parameter w [16] may allow the accommodation of such bigger masses at the cost of assuming $w < -1$ and a lower expansion age of the universe, as recently remarked in [17].

[2]Another (possibly coexisting) realization is provided by new sterile species separated from the active ones by extremely small mass-squared splittings [20,21]. However, such schemes do not have observable effects in VSBL settings and we do not consider them in this work.

[3]The solar data are insensitive to the reciprocal ordering of the third and fourth mass eigenstates, as well as to their ordering respect to the doublet (ν_1, ν_2). In this work we assume for definiteness $m_1 < m_2 < m_3 < m_4$, always referring to the positive mass-squared splittings defined as $\Delta m_{ij}^2 = m_j^2 - m_i^2$ $(i < j)$.

with the new mass eigenstates, the $3 + s$ schemes leave basically unaltered also the standard oscillation amplitudes, thus realizing a genuine perturbation of the leading 3-flavor scenario, whose size must respect the constraints imposed by all the existing phenomenology.[4]

The solar sector (Solar and KamLAND data) has had a pivotal role in establishing and shaping the 3-flavor framework and continue to be of extreme importance in sharpening its basic parameters. As a matter of fact, these data are the only ones sensitive to the admixture of the electron neutrino with the first two mass eigenstates (ν_1, ν_2), also possessing a subleading sensitivity to the (averaged) ν_3-driven oscillations. This translates into stringent constraints on the amplitude of the elements (U_{e1}, U_{e2}, U_{e3}) entering the first row of the lepton mixing matrix. Therefore, it is of certain interest to explore how such a sector "responds" to the perturbations generated by a nonzero mixing of the electron neutrino with new sterile species, as hinted at by the recent VSBL findings.

The impact of new sterile species on the phenomenology of the solar neutrino sector has been investigated in several works, both as a leading mechanism [26,27] (in the "pre-KamLAND era") and as a subdominant one [28–34] (after the KamLAND results). However, all the existing analyses[5] have been performed in the simplified framework—whose formalism was originally developed in [35]—of pure (ν_1-ν_2)-driven oscillations, which neglects the possible mixing of the electron neutrino with the third standard mass eigenstate ($U_{e3} = 0$) and with a new fourth one ($U_{e4} = 0$). In the past, both assumptions were justified by the limited sensitivity of this data set and by the strong upper bounds put on these matrix elements by the reactor experiments performed with short [36] (sensitive to U_{e3}) and very short [37] (sensitive to U_{e4}) baselines. Moreover, no hint of transitions into sterile states was evidenced in the aforementioned analyses, so there was no reason to extend them beyond such a simple scheme. However, this situation has gradually changed in the recent years. On the one hand, we have witnessed a substantial increase in the sensitivity of the solar sector to possible departures from the simple 2-flavor approximation; the recent indication of $\theta_{13} > 0$ [38] and the possible hint of nonstandard MSW dynamics [39] (see also [40]) suggested by these data testify such a new trend. On the other hand, the new anomalies directly point towards a relatively big amplitude of U_{e4}, which should be now testable at the solar sector.

The incorporation of the $3 + s$ schemes in the description of solar neutrino conversions is not a trivial task, however, as it requires the treatment of the MSW effect in the presence of sterile species. This problem has been recently addressed in [41], where a parameterization independent form of the lepton mixing matrix has been exploited, and selected numerical examples have been given for the relevant transition probabilities. In this work we make a step forward and, by adopting a convenient parameterization of the mixing matrix, we put quantitative constraints on these schemes, focusing on the electron neutrino mixing. The rest of our paper is organized as follows. In Sec. II, we introduce the $3 + 1$ neutrino framework and present the basic formulae needed to interpret the flavor oscillations in vacuum and in (solar) matter within such a scheme. In Sec. III, we discuss the results of the numerical analysis, drawing our conclusions in Sec. IV. Four Appendices address the following (more technical) issues: A The treatment of the solar MSW effect in a $3 + 1$ scheme; B Its generalization to the $3 + s$ frameworks; C The incorporation of Earth-induced matter effects; D The potential sensitivity of solar neutrino flavor transitions to the Dirac CP-violating phases entering the 4-lepton mixing matrix.

[4]This includes the atmospheric neutrino data collected at neutrino telescopes [22], where the new sterile species may leave distinctive imprints [23–25].

[5]An exception is constituted by the work [30], where a qualitative discussion of the impact of nonzero U_{e3} is provided.

II. FRAMEWORK AND BASIC ANALYTICAL RESULTS

A. Parameterization of the mixing matrix

In the presence of a fourth sterile neutrino ν_s, the flavor (ν_α, $\alpha = e, \mu, \tau, s$) and the mass eigenstates (ν_i, $i = 1, 2, 3, 4$), are connected through a 4×4 unitary mixing matrix U, which depends on six complex parameters [42]. Such a matrix can thus be expressed as the product of six complex elementary rotations, which define six real mixing angles and six CP-violating phases. Of the six phases three are of the Majorana type and are unobservable in oscillation processes, while the three remaining ones are of the Dirac type. For simplicity, in this work, we set to zero all the Dirac phases, commenting only in Appendix D on the potential sensitivity of the solar data to them.

As it will appear clear in what follows, for the treatment of the solar MSW transitions under study, it is convenient to parameterize the mixing matrix as

$$U = R_{23}R_{24}R_{34}R_{14}R_{13}R_{12} \equiv BR_{14}R_{13}R_{12} \equiv AR_{12}, \quad (1)$$

where R_{ij} represents a real 4×4 rotation in the (i, j) plane containing the 2×2 submatrix

$$R_{ij}^{2\times 2} = \begin{pmatrix} c_{ij} & s_{ij} \\ -s_{ij} & c_{ij} \end{pmatrix} \quad (2)$$

in the (i, j) sub-block, with ($c_{ij} \equiv \cos\theta_{ij}$, $s_{ij} \equiv \sin\theta_{ij}$), and the matrices $A \equiv UR_{12}^T$ and $B \equiv R_{23}R_{24}R_{34}$ have been introduced for later convenience.

The parameterization in Eq. (1) has the following properties: (I) For vanishing mixing involving the fourth state ($\theta_{14} = \theta_{24} = \theta_{34} = 0$) Eq. (1) reduces to the 3-flavor mixing matrix in its standard parameterization [43]; (II) The leftmost positioning of the matrix R_{23} allows us to rotate away the mixing angle θ_{23} from the solar MSW dynamics (see Appendix A) and from the expression of the mixing elements involving the sterile flavor (see the discussion below); (III) The positioning of the product $R_{14}R_{13}$ close to the rightmost matrix R_{12} makes the corresponding mixing angles appear in a symmetrical way in the expressions of the admixtures of the electron neutrino with the (ν_1, ν_2) mass eigenstates, inducing small admixtures with the far (ν_3, ν_4) mass eigenstates, which in the limit of small θ_{14} also appear in a symmetrical form, being $U_{e3}^2 \simeq \sin^2\theta_{13}$ and $U_{e4}^2 = \sin^2\theta_{14}$. In fact, the mixing matrix elements involving the electron neutrino are expressed as

$$U_{e1} = A_{11}c_{12} - A_{12}s_{12}, \tag{3}$$

$$U_{e2} = A_{11}s_{12} + A_{12}c_{12}, \tag{4}$$

$$U_{e3} = A_{13}, \tag{5}$$

$$U_{e4} = A_{14}, \tag{6}$$

in terms of the elements of the first row of the matrix A. The rightmost positioning of the product $R_{14}R_{13}R_{12}$ in such a matrix ensures that its element A_{12} is equal to zero, thus leading to the explicit expressions

$$U_{e1} = c_{14}c_{13}c_{12}, \tag{7}$$

$$U_{e2} = c_{14}c_{13}s_{12}, \tag{8}$$

$$U_{e3} = c_{14}s_{13}, \tag{9}$$

$$U_{e4} = s_{14}. \tag{10}$$

It should be noted that these expressions are not affected by the premultiplication of the matrix B in Eq. (1), since this induces a rotation in the hyperplane orthogonal to the axis with index $i = 1$, and therefore are independent of the specific order of the three matrices (R_{23}, R_{24}, R_{34}). Since the solar data are sensitive also to transitions into sterile neutrinos, we will need the expressions of the matrix elements involving the sterile flavor, which, taking into account the last equality in Eq. (1), can be written as

$$U_{s1} = A_{41}c_{12} - A_{42}s_{12}, \tag{11}$$

$$U_{s2} = A_{41}s_{12} + A_{42}c_{12}, \tag{12}$$

$$U_{s3} = A_{43}, \tag{13}$$

$$U_{s4} = A_{44}, \tag{14}$$

in terms of the elements of the fourth row of the matrix A, which in our parameterization have the explicit expressions

$$A_{41} = c_{24}(s_{34}s_{13} - c_{34}s_{14}c_{13}), \tag{15}$$

$$A_{42} = -s_{24}, \tag{16}$$

$$A_{43} = -c_{24}(s_{34}c_{13} + c_{34}s_{14}s_{13}), \tag{17}$$

$$A_{44} = c_{24}c_{34}c_{14}, \tag{18}$$

independent of the mixing angle θ_{23}, due to the leftmost positioning of the matrix R_{23} in the definition of the mixing matrix in Eq. (1). The relations in Eq. (11)–(18) also evidence the following further features of our parameterization: (IV) For small values of all the mixing angles involving the fourth mass eigenstate [$s_{i4}^2 \ll 1$ ($i =$ 1, 2, 3)], the sterile flavor content is mostly distributed on the fourth mass eigenstate ($U_{s4} \simeq 1$); (V) For $\theta_{13} \simeq \theta_{14} \simeq 0$, the sterile content of the first two mass eigenstates essentially depends only on θ_{24}, being in this limit $U_{s1}^2 + U_{s2}^2 \simeq A_{42}^2 = s_{24}^2$; (VI) For $\theta_{13} \simeq \theta_{14} \simeq \theta_{24} \simeq 0$, the mixing angle θ_{34} basically exchanges the amplitude of U_{s3} with that of U_{s4}.

It should be stressed that our parameterization—"tailored" for the solar sector—is different from that commonly adopted for the 4-flavor analyses of the atmospheric and long baseline neutrino data [44,45]. In such a case, the mixing matrix is still taken of the form $U = BR_{14}R_{13}R_{12}$ but with a different choice of the ordering of the rotations entering B ($B_{\rm atm} \equiv R_{34}R_{24}R_{23}$), which is dictated by the fact that $\nu_\mu \to \nu_\tau$ transitions are sensitive to the matrix elements connecting ν_μ and ν_τ to the new mass eigenstate ν_4. Indeed, with such a choice, in the limit of small admixtures with the fourth state, one has the approximate expressions $s_{24}^2 \simeq U_{\mu 4}^2$ and $s_{34}^2 \simeq U_{\tau 4}^2$. In this regard, we observe that the parameterization we have adopted could be classified as of a "mixed form" in between the two ones recognized in [33] as more apt for studying those data sets possessing, respectively, a prevailing sensitivity to admixtures (of the new state $\nu_s \sim \nu_4$) with the flavor eigenstates ($U_{\alpha 4} \neq 0$) or with the mass ones ($U_{si} \neq 0$). Such a particular form ensues from the peculiar properties of the solar sector data, which are sensitive both to U_{e4} ("favor-type" admixture) and to the U_{si}'s ("mass-type" admixtures).

B. Four-flavor evolution

The evolution of the neutrino flavor eigenstates is governed by the Schrödinger-like equation

$$i\frac{d}{dx}\begin{pmatrix}\nu_e\\ \nu_\mu\\ \nu_\tau\\ \nu_s\end{pmatrix} = H_f\begin{pmatrix}\nu_e\\ \nu_\mu\\ \nu_\tau\\ \nu_s\end{pmatrix}, \tag{19}$$

where the Hamiltonian

$$H_f = H_f^{\rm kin} + H_f^{\rm dyn} = UKU^T + V(x) \tag{20}$$

has been split in the sum of a kinematical and a dynamical term. In Eq. (20) K denotes the diagonal matrix containing the wave numbers ($k_i = m_i^2/2E$ $i = 1, 2, 3, 4$) (m_i and E being the neutrino mass-squared and energy, respectively), while the matrix $V(x)$ incorporates the matter MSW potential [46,47]. Barring irrelevant factors proportional to the identity, we can define the diagonal matrix containing the three relevant wave numbers as

$$K = \mathrm{diag}(0, k_{\mathrm{sol}}, k_{\mathrm{atm}}, k_{\mathrm{new}}) \tag{21}$$

$$\equiv \mathrm{diag}\left(0, \frac{\Delta m_{21}^2}{2E}, \frac{\Delta m_{31}^2}{2E}, \frac{\Delta m_{41}^2}{2E}\right)$$

and the matrix encoding the matter effects, as

$$V = \mathrm{diag}(V_{\mathrm{CC}}, 0, 0, -V_{\mathrm{NC}}), \tag{23}$$

where

$$V_{\mathrm{CC}} = \sqrt{2} G_F N_e(x) \tag{24}$$

is the charged-current interaction potential of the electron neutrinos with the background electrons having number density N_e, and

$$V_{\mathrm{NC}} = -\frac{1}{2}\sqrt{2} G_F N_n(x) \tag{25}$$

is the neutral-current interaction potential (common to all the active neutrino species) with the background neutrons having number density N_n. For later convenience, we also introduce the position-dependent parameter $r_x \equiv r(x)$ defined as the positive-definite ratio

$$r_x = -\frac{V_{\mathrm{NC}}(x)}{V_{\mathrm{CC}}(x)} = \frac{1}{2}\frac{N_n(x)}{N_e(x)}. \tag{26}$$

C. Oscillation probabilities in vacuum

In the case of propagation in vacuum, Eq. (19) leads to the survival probability of electron (anti-)neutrinos (which is relevant for the reactor experiment KamLAND[6])

$$P_{ee} = 1 - 4\sum_{j>k} U_{ej}^2 U_{ek}^2 \sin^2\phi_{jk}, \tag{27}$$

with the elements $U_{ei} (i = 1, \ldots, 4)$ determining the amplitudes of the oscillating terms having phases $\phi_{jk} = \Delta m_{jk}^2 L/4E$ developed over the baseline L. In the hierarchical limit $k_{\mathrm{sol}} \ll k_{\mathrm{atm}} \ll k_{\mathrm{new}}$ the fast oscillations induced by the two larger wave numbers are completely averaged and the survival probability can be written as

$$P_{ee} = \left(1 - \sum_{k=3}^{4} U_{ek}^2\right)^2 P_{ee}^{2\nu} + \sum_{k=3}^{4} U_{ek}^4, \tag{28}$$

where

$$P_{ee}^{2\nu} = 1 - 4 s_{12}^2 c_{12}^2 \sin^2\phi_{12} \tag{29}$$

is the well known 2-flavor expression of the survival probability in vacuum. Equation (28) shows that the presence of the far eigenstates ν_3 and ν_4 is felt as a lack of unitarity of the (ν_1, ν_2) sector and that there is an exact degeneracy between U_{e3} and U_{e4}. In our parameterization of the mixing matrix Eq. (28) reads

$$P_{ee} = c_{14}^4 c_{13}^4 P_{ee}^{2\nu} + c_{14}^4 s_{13}^4 + s_{14}^4, \tag{30}$$

which implies an approximate degeneracy between the two (small) mixing angles θ_{13} and θ_{14}.

D. Transition probabilities in matter

Matter effects play a central role in the conversion of solar neutrinos and should be incorporated following the treatment presented in Appendix A. It must be observed that, although the solar data are mainly sensitive to the survival probability of the electron neutrinos, they also posses a sensitivity to the transition probability into sterile states (P_{es}) through the neutral current (NC) measurements performed by the SNO experiment and, to a lesser extent, through the elastic scattering (ES) interactions exploited by Super-Kamiokande and Borexino.

As shown in Appendix A, for the small values of the two mixing angles θ_{13} and θ_{14} we are considering, the propagation of solar neutrinos is adiabatic, and the transition probabilities only depend upon their production and detection points. Neglecting Earth-induced matter effects[7] one has the general expressions

$$P(\nu_e \to \nu_\alpha) = \sum_{i=1}^{4} U_{\alpha i}^2 (U_{ei}^m)^2 \qquad (\alpha = e, \mu, \tau, s), \tag{31}$$

where the U_{ei}^m's denote the mixing matrix elements involving the electron neutrino in the production point. As shown in Appendix A, in our parameterization these elements can be simply obtained by replacing in Eqs. (7)–(10) the mixing angle θ_{12} in vacuum with the corresponding one in matter

$$U_{e1}^m = c_{14} c_{13} c_{12}^m, \tag{32}$$

$$U_{e2}^m = c_{14} c_{13} s_{12}^m, \tag{33}$$

$$U_{e3}^m = U_{e3} = c_{14} s_{13}, \tag{34}$$

$$U_{e4}^m = U_{e4} = s_{14}, \tag{35}$$

where θ_{12}^m can be calculated using the prescriptions provided in Eqs. (A18)–(A20). In the numerical analysis we are going to present in this work, we will limit ourselves to

[6] In this discussion we neglect the small matter effects induced by the interaction of the electron antineutrinos with the Earth crust. However, for the sake of precision, we include these effects in the numerical analysis presented in the next section.

[7] Here, for simplicity, we neglect Earth matter effects which, however, are properly included in the numerical analysis following the prescription described in Appendix C.

the simple case $\theta_{24} = \theta_{34} = 0$. In this case, the matrix A in Eq. (1) takes the simpler form $A = R_{23}R_{14}R_{13}$, implying the following simplified expressions for the mixing elements involving the sterile flavor

$$U_{s1} = -s_{14}c_{13}c_{12}, \tag{36}$$

$$U_{s2} = -s_{14}c_{13}s_{12}, \tag{37}$$

$$U_{s3} = -s_{14}s_{13}, \tag{38}$$

$$U_{s4} = c_{14}, \tag{39}$$

which show that, in this case, the small departure from unity of the sterile flavor content of the fourth mass eigenstate is redistributed (by unitarity) essentially to the first two mass eigenstates, leaving $U_{s3}^2 \sim 0$. Using Eqs. (A18)–(A20), one arrives at the expressions

$$P_{ee} = c_{14}^4 c_{13}^4 \bar{P}_{ee}^{2\nu} + c_{14}^4 s_{13}^4 + s_{14}^4, \tag{40}$$

$$P_{es} = c_{14}^2 s_{14}^2 c_{13}^4 \bar{P}_{ee}^{2\nu} + c_{14}^2 s_{14}^2 s_{13}^4 + c_{14}^2 s_{14}^2, \tag{41}$$

where

$$\bar{P}_{ee}^{2\nu} = c_{12}^2 (c_{12}^m)^2 + s_{12}^2 (s_{12}^m)^2 \tag{42}$$

is the well known expression of the 2-flavor survival probability in the adiabatic regime [48] but with the mixing angle θ_{12}^m obtained using the rescaled charged-current potential $V_{CC} \to (c_{14}^2 + r_x s_{14}^2) c_{13}^2 V_{CC}$ (see Appendix A). In the case of $\theta_{14} = 0$, Eqs. (40) and (41) return the standard 3-flavor expressions [49,50]

$$P_{ee}^{3\nu} = c_{13}^4 \bar{P}_{ee}^{2\nu} + s_{13}^4, \tag{43}$$

$$P_{es}^{3\nu} = 0, \tag{44}$$

with the well known rescaling of the standard MSW potential $V_{CC} \to c_{13}^2 V_{CC}$ [49,50]. Conversely, in the case ($\theta_{13} = 0$, $\theta_{14} \neq 0$), one gets

$$P_{ee}(\theta_{13} = 0) = c_{14}^4 \bar{P}_{ee}^{2\nu} + s_{14}^4, \tag{45}$$

$$P_{es}(\theta_{13} = 0) = c_{14}^2 s_{14}^2 (\bar{P}_{ee}^{2\nu} + 1), \tag{46}$$

with the rescaled potential $V_{CC} \to (c_{14}^2 + r_x s_{14}^2) V_{CC}$. We observe that, while the form of the electron neutrino survival probability is identical to that obtained in the 3-flavor case, modulo the replacement $\theta_{13} \to \theta_{14}$ and a small change in the rescaling factor of the potential, in this case, there is a nonzero transition probability into sterile states. In all cases, the change in the potential is very small, and, analogously to the 3-flavor limit [51], it introduces only a mild (undetectable) energy dependence of the (significant) energy-independent suppression induced by the kinematical factor $c_{14}^4 c_{13}^4 \sim 1 - 2s_{14}^2 - 2s_{13}^2$ appearing in Eq. (40).

III. NUMERICAL RESULTS

In our analysis we have included the data from the Chlorine (Cl) experiment [52], the Gallium (Ga) detectors SAGE [53] and GALLEX/GNO [54–56], Super-Kamiokande [57] (SK), all the three phases of the Sudbury Neutrino Observatory [58–61] (SNO), and Borexino [62,63] (BX). We have not included the spectral information provided by the SNO Low Energy Threshold Analysis [64], since this can be used only under the assumption of unitary conversion among the active neutrino species ($P_{ee} + P_{e\mu} + P_{e\tau} = 1$), which is violated in the presence of transitions into new sterile states. For the sake of precision, we have also incorporated the small Earth-induced matter effects, following the treatment presented in Appendix C. Concerning KamLAND, we have included in our analysis the latest data released in [65]. For definiteness, we have adopted the new improved reactor flux determinations [1]. All plots will refer to this case, and, when appropriate, we will comment in the text on the differences that would arise with a different choice of the reactor fluxes. In all numerical computations we have set $\theta_{24} = \theta_{34} = 0$, commenting at the end of the Section on the possible role of these parameters. Therefore, the parameter space spanned by our analysis will involve the solar mass spliting Δm_{12}^2 and the three mixing angles (θ_{12}, θ_{13}, θ_{14}).

We start our numerical study considering the familiar three-flavor case ($\theta_{13} \neq 0$, $\theta_{14} = 0$), in which the results of the analysis depend on the three parameters (Δm_{12}^2, θ_{12}, θ_{13}). This case will serve as a useful term of comparison for the more general results of the 4ν analysis. In the left panel of Fig. 1 we show the region allowed by solar (S) and KamLAND (K) in the plane spanned by the two mixing angles, having marginalized away the solar mass splitting in the region determined by KamLAND. Respect to previous analyses [38,65–69], the KamLAND data *taken*

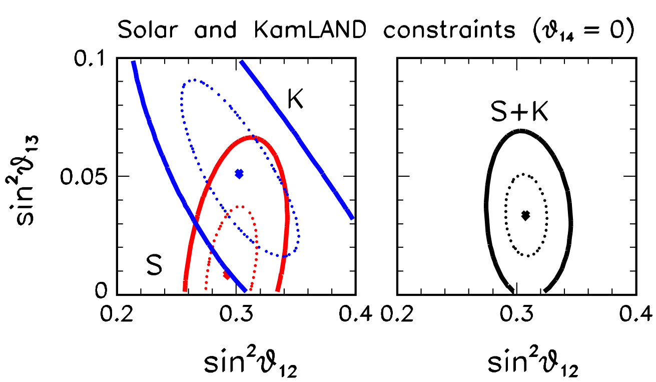

FIG. 1 (color online). Region allowed in the [$\sin^2\theta_{12}$, $\sin^2\theta_{13}$] plane for $\theta_{14} = 0$, after marginalization of Δm_{12}^2 as constrained by KamLAND, separately (left panel) by solar (S) and KamLAND (K) data and by their combination (right panel). In both panels it has been set $\theta_{24} = \theta_{34} = 0$. The contours refer to $\Delta\chi^2 = 1$ (dotted line) and $\Delta\chi^2 = 4$ (solid line).

alone now tend to prefer values of $\theta_{13} > 0$ (see also [6,70]). This behavior can be traced to our adoption of the new (higher) reactor fluxes [1]. In fact, according to Eq. (43), a larger value of θ_{13} is now required to suppress the bigger total rate induced by the new higher fluxes. Furthermore, similarly to previous analyses [38,65–69], for $\theta_{13} > 0$ the values of the mixing angle θ_{12} identified by the solar and KamLAND experiments are in better agreement due to the opposite-leaning correlations exhibited by their respective contours, giving rise to an enhanced preference for nonzero θ_{13} in their combination (right panel). We find that the 2-flavor case ($\theta_{13} = 0$) is disfavored at the 1.8σ level (which is reduced to 1.3σ using the old reactor fluxes).

As a second step we switch on only the mixing angle θ_{14}, setting $\theta_{13} = 0$. In this case, the results of the analysis depend on the three parameters (Δm^2_{12}, θ_{12}, θ_{14}), whose allowed regions are displayed in Fig. 2. As discussed in Sec. II, KamLAND cannot distinguish θ_{13} from θ_{14}, and, as a result, the region identified by such an experiment is identical to that found in the 3-flavor case. In contrast, the region determined by the solar data is slightly different from the corresponding one identified in the 3-flavor case. In particular, we see that the correlation in the $[s^2_{12}, s^2_{14}]$ plane is different from that exhibited in the $[s^2_{12}, s^2_{13}]$ plane. To understand this point, it is useful to write the relations connecting the total fluxes observed in the solar neutrino experiments to the electron neutrino survival probability and their transition probability into sterile states. Taking into account that $P_{ee} + P_{e\mu} + P_{e\tau} + P_{es} = 1$, we have

$$\phi^{\rm CC} = \Phi_B \langle P_{ee} \rangle, \qquad (47)$$

$$\phi^{\rm ES} = \Phi_B (\langle P_{ee} \rangle + r_\sigma (1 - \langle P_{ee} \rangle - \langle P_{es} \rangle)), \qquad (48)$$

$$\phi^{\rm NC} = \Phi_B (1 - \langle P_{es} \rangle), \qquad (49)$$

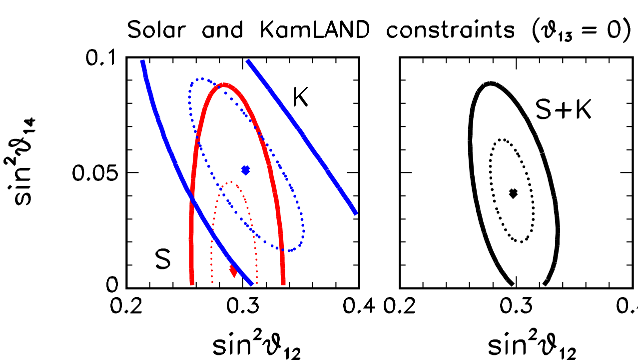

FIG. 2 (color online). Region allowed in the $[\sin^2\theta_{12}, \sin^2\theta_{14}]$ plane for $\theta_{13} = 0$, after marginalization of Δm^2_{12} as constrained by KamLAND, separately (left panel) by solar (S) and KamLAND (K) data and by their combination (right panel). In both panels it has been set $\theta_{24} = \theta_{34} = 0$. The contours refer to $\Delta\chi^2 = 1$ (dotted line) and $\Delta\chi^2 = 4$ (solid line).

where Φ_B is the solar ^8B neutrino flux expected in the absence of oscillations, while $\phi^{\rm X}$ (X = CC, ES, NC) is the flux expected in charged-current (CC), ES, and NC reactions. The symbol $\langle\rangle$ denotes the average over appropriate response functions [71,72], which depend on the experiment and on the specific reaction considered. We remind that: (I) The radiochemical experiments (Cl, Ga) employ a CC absorption reaction and are thus sensitive only to P_{ee}; (II) The BX and SK detectors make use of an ES reaction and can probe also P_{es}, although with sensitivity reduced by the small ratio $r_\sigma \sim 1/6$ of the energy-averaged ES cross-sections of $\nu_{\mu,\tau}$ and ν_e; (III) The SNO experiment detects the solar neutrinos using all the three reactions (CC, ES, NC), thus possessing a pronounced sensitivity to P_{es} through the NC process.

In the 3-flavor case, the sensitivity of the solar data taken alone to the mixing angle θ_{13} arises from an interplay of low-energy (LE) and high-energy (HE) (essentially the SNO CC/NC ratio) data [73,74], engendered by a different dependence of the survival probability on the two mixing angles θ_{12} and θ_{13} in the two regimes. From Eqs. (47)–(49), taking into account that in the LE (vacuum-like) regime $\bar{P}^{2\nu}_{ee} \sim 1 - 2s^2_{12}c^2_{12}$ and in the HE (matter-dominated) regime $\bar{P}^{2\nu}_{ee} \sim s^2_{12}$, and using Eq. (43), we have the following relations for the LE and HE fluxes

$$\phi^{\rm CC}_{\rm LE} \propto P^{\rm LE}_{ee} \simeq (1 - 2s^2_{13})(1 - 2s^2_{12}c^2_{12}), \qquad (50)$$

$$\left[\frac{\phi^{\rm CC}}{\phi^{\rm NC}}\right]_{\rm HE} \simeq P^{\rm HE}_{ee} \simeq (1 - 2s^2_{13})s^2_{12}. \qquad (51)$$

The different relative sign of the two factors proportional to s^2_{13} and s^2_{12} in Eqs. (50) and (51) gives rise to an opposite correlation among these two parameters, providing an enhanced sensitivity to small departures from zero of the mixing angle θ_{13}. Since the SNO CC/NC ratio is measured with better precision than the LE flux (essentially provided by the Ga experiments), the negative relative sign in Eq. (51) prevails in the global fit, giving rise to the positive overall correlation among the two mixing angles appearing in the left panel of Fig. 1 in the curve designed with label "S". Indeed, according to Eq. (51), a bigger value of θ_{13} is needed to counterbalance the effect of a larger θ_{12}, in order to keep the CC/NC ratio at the fixed value determined by the SNO experiment.

In the case of $\theta_{14} \neq 0$, while we have an identical expression for the expected flux in the LE limit (modulo the replacement $\theta_{13} \rightarrow \theta_{14}$), the SNO CC/NC ratio depends also on P_{es}. For small values of θ_{14}, using Eqs. (45) and (46), we have

$$\phi^{CC}_{\rm LE} \propto P^{\rm LE}_{ee} \simeq (1 - 2s^2_{14})(1 - 2s^2_{12}c^2_{12}), \qquad (52)$$

$$\left[\frac{\phi^{\rm CC}}{\phi^{\rm NC}}\right]_{\rm HE} \simeq P^{\rm HE}_{ee}(1 + P^{\rm HE}_{es}) \simeq (1 - c^2_{12}s^2_{14})s^2_{12}. \qquad (53)$$

In this case the coefficient in front of the product $s_{14}^2 s_{12}^2$ in the SNO CC/NC ratio is still negative but 3 times smaller ($c_{12}^2 \sim 0.7$) than the corresponding one appearing in the 3-flavor expression. As a result, in such a case, the synergetic effect of the combination LE and HE data slightly decreases, with a lower sensitivity to θ_{14} and a weak negative overall correlation in the $[s_{12}^2, s_{14}^2]$ plane (see the curve designed with label S in the left panel of Fig. 2), as now the LE data can compete with the HE ones in determining the relative sign in front of the product $s_{14}^2 s_{12}^2$. Similarly to the 3-flavor case, the values of the mixing angle θ_{12} identified, respectively, by solar and KamLAND are in better agreement for $\theta_{14} > 0$, with an enhanced preference for nonzero values of this parameter in their combination (right panel in Fig. 2). Also in this case we find that $\theta_{14} = 0$ is disfavored at the 1.8σ level (which is reduced to 1.3σ using the old reactor fluxes).

The following small differences appear between the two cases: (I) A weaker upper bound on θ_{14} ($s_{14}^2 < 0.089$ at the 2σ level) with respect to that obtained for θ_{13} ($s_{13}^2 < 0.070$ at the 2σ level); (II) A slightly bigger best fit value for θ_{14} ($s_{14}^2 = 0.041$) with respect to that obtained for θ_{13} ($s_{13}^2 = 0.033$). It is interesting to note that the best fit value obtained for θ_{14} practically coincides with that indicated by the VSBL reactor and Gallium calibration anomalies taken in combination [6]. Therefore, combining the solar sector results with such data would reinforce their preference for nonzero θ_{14}, providing an overall indication, which we roughly estimate to be around the $\sim 4\sigma$ level.

As a third step of our numerical analysis, we have switched on both mixing angles ($\theta_{13} \neq 0$, $\theta_{14} \neq 0$). In Fig. 3 we show the region allowed by the combination of solar and KamLAND in the plane spanned by such two parameters, having marginalized away both the mass splitting Δm_{12}^2 and the mixing angle θ_{12}. From this plot we see that there is a complete degeneracy among the two parameters. In practice, this data set is basically sensitive to the combination $U_{e3}^2 + U_{e4}^2$, the small deviations from this behavior being induced by the SNO NC measurement. Therefore, the solar sector data, while indicating a weak preference for nonzero admixture of the electron neutrino with the far mass eigenstates ν_3 and ν_4, cannot distinguish between them. The same conclusion holds true if additional sterile neutrinos are considered, as shown in Appendix B.

We conclude this section with a final remark. As in our analysis we have set $\theta_{24} = \theta_{34} = 0$, the question arises as to whether a nonzero value of such parameters can alter the basic conclusions of the analysis. With this purpose, we have performed the analysis considering this possibility, and we have found that, although the correlations observed in Figs. 1 and 2 can slightly change, the degeneracy among the two parameters θ_{13} and θ_{14} persists, as one may have expected, since the additional freedom given to the system can only worsen its preexisting degeneracies. We postpone to a future work the investigation of the constraints attainable on the mixing angles θ_{24} and θ_{34}, noticing that in this case one should take into account the (small) effects of the CP violating phases entering the lepton mixing matrix, as discussed in Appendix D.

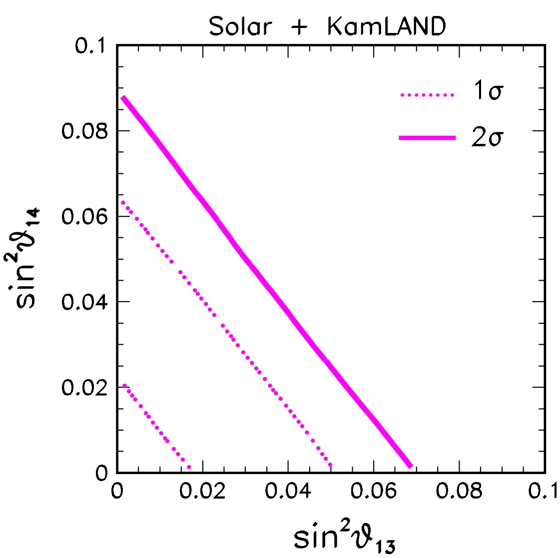

FIG. 3 (color online). Region allowed, after marginalization of Δm_{12}^2 and θ_{12}, by the combination of solar and KamLAND data (for $\theta_{24} = \theta_{34} = 0$). The contours refer to $\Delta\chi^2 = 1$ (dotted line) and $\Delta\chi^2 = 4$ (solid line).

IV. CONCLUSIONS

Motivated by the recent experimental findings which point towards the existence of new light sterile neutrino species, we have explored their impact on the solar sector phenomenology. Working in a CPT-conserving $3 + 1$ scheme, we have considered the perturbations induced by a non-negligible mixing of the electron neutrino with a fourth sterile neutrino specie. Our quantitative analysis shows that the present data posses a sensitivity to the amplitude of the lepton mixing matrix element U_{e4}, which is comparable to that achieved on the standard matrix element U_{e3}. In addition, our analysis evidences that, in a 4-flavor framework, the current preference for $|U_{e3}| \neq 0$ is indistinguishable from that for $|U_{e4}| \neq 0$, having both a similar statistical significance (which is $\sim 1.3\sigma$ adopting the old reactor fluxes determinations and $\sim 1.8\sigma$ using their new estimates.) Such a degeneracy naturally extends to the more general $3 + s$ schemes, implying that in these frameworks, the present hint for nonzero θ_{13} must be reinterpreted as a preference for a nonzero mixing of the electron neutrino with mass eigenstates distant from the (ν_1, ν_2) doublet. Different kinds of probes are needed in order to discriminate whether such an admixture—if effectively confirmed to be nonzero—is realized with the third standard mass eigenstate ν_3 or with new neutrino specie(s).

ACKNOWLEDGMENTS

We are grateful to J. W. F. Valle for stimulating exchanges of ideas held at the Instituto de Física Corpuscular in Valencia, where this work was initiated. We also thank E. Lisi, G. G. Raffelt, and A. Yu. Smirnov for precious discussions and A. M. Rotunno for useful information on the KamLAND data analysis. We thank the organizers of the *46th Rencontres de Moriond on Electroweak Interactions and Unified Theories* held in La Thuile—where preliminary results of this work were presented—for kind hospitality. Our work is supported by the DFG Cluster of Excellence on the ''Origin and Structure of the Universe''.

APPENDIX A: THE MSW EFFECT IN A 3 + 1 SCHEME

To treat the MSW effect in a 3 + 1 scheme it is convenient to introduce the new basis

$$\bar{\nu} = A^T \nu, \tag{A1}$$

where

$$A = R_{23} R_{24} R_{34} R_{14} R_{13} \equiv U R_{12}^T \tag{A2}$$

is the same matrix defined in Eq. (1). In this new basis the Hamiltonian assumes the form

$$\bar{H} = \bar{H}^{\rm kin} + \bar{H}^{\rm dyn} = R_{12} K R_{12}^T + A^T V A, \tag{A3}$$

and, in the hierarchical limit $k_{\rm sol} \ll k_{\rm atm} \ll k_{\rm new}$, similarly to the 3-flavor case [48], one can reduce the dynamics to that of an effective 2ν system. Indeed, from Eq. (A3) one has that the (3, 3) and (4, 4) entries of $\bar{H}$, being proportional to $k_{\rm atm}$ and $k_{\rm new}$, are much bigger than all the other ones, and at the zeroth order in the small quantities $V_{\rm CC}/k_{\rm atm}$, $V_{\rm NC}/k_{\rm atm}$, $V_{\rm CC}/k_{\rm new}$, $V_{\rm NC}/k_{\rm new}$, the third and fourth eigenvalues of $\bar{H}$ are much larger than the first two ones. As a result, the states $\bar{\nu}_3 = \nu_3$ and $\bar{\nu}_4 = \nu_4$ evolve independent one of each other and, more importantly, completely decoupled from $\bar{\nu}_1$ and $\bar{\nu}_2$. Extracting from $\bar{H}$ the submatrix with indices (1, 2) one obtains the 2 × 2 Hamiltonian

$$\bar{H}_{2\nu} = \bar{H}_{2\nu}^{\rm kin} + \bar{H}_{2\nu}^{\rm dyn}, \tag{A4}$$

governing the evolution of the $(\bar{\nu}_1, \bar{\nu}_2)$ system, whose dynamical part has the form

$$\bar{H}_{2\nu}^{\rm dyn} = V_{\rm CC}(x) \begin{pmatrix} A_{11}^2 + r_x A_{41}^2 & A_{11}A_{12} + r_x A_{41} A_{42} \\ A_{11}A_{12} + r_x A_{41} A_{42} & A_{12}^2 + r_x A_{42}^2 \end{pmatrix}. \tag{A5}$$

In our parameterization the rotation R_{23} appears as the leftmost matrix in A, and therefore the product $A^T V A$ does not depend on θ_{23} since R_{23} commutes with the matrix V of the potential given in Eq. (23). Furthermore, the matrix A contains the product $R_{14} R_{13}$ as its rightmost factor, implying that its element A_{12} is equal to zero. Therefore, the 2 × 2 Hamiltonian in Eq. (A5) can be recast in the form

$$\bar{H}_{2\nu}^{\rm dyn} = V_{\rm CC}(x) \begin{pmatrix} \gamma^2 + r_x \alpha^2 & r_x \alpha\beta \\ r_x \alpha\beta & r_x \beta^2 \end{pmatrix}, \tag{A6}$$

where the parameters (α, β, γ) are defined as

$$\alpha = A_{41} = c_{24}(s_{34} s_{13} - c_{34} s_{14} c_{13}), \tag{A7}$$

$$\beta = A_{42} = -s_{24}, \tag{A8}$$

$$\gamma = A_{11} = c_{13} c_{14}, \tag{A9}$$

which, according to Eqs. (11)–(14), are related to the mixing matrix elements as follows

$$U_{s1} = \alpha c_{12} - \beta s_{12}, \tag{A10}$$

$$U_{s2} = \alpha s_{12} + \beta c_{12}, \tag{A11}$$

showing that the sum of α^2 and β^2 represents the sterile content of the (ν_1, ν_2) doublet

$$\alpha^2 + \beta^2 = U_{s1}^2 + U_{s2}^2. \tag{A12}$$

Furthermore, using Eqs. (3)–(10) we have

$$\gamma^2 = U_{e1}^2 + U_{e2}^2 = 1 - U_{e3}^2 - U_{e4}^2. \tag{A13}$$

It is instructive to consider the following limit cases:

(I) For vanishing mixing with the fourth neutrino specie ($\theta_{14} = \theta_{24} = \theta_{34} = 0$) one has $\alpha = \beta = 0$ and $\gamma = c_{13}$, thus recovering the standard 3-flavor result [49,50], in which the admixture with the third state ν_3 induces the simple rescaling of the potential $V_{\rm CC} \to c_{13}^2 V_{\rm CC}$;

(II) When only the mixing angle θ_{14} is different from zero, $\alpha = -s_{14}$, $\beta = 0$, and $\gamma = c_{14}$, with the position-dependent rescaling of the standard potential $V_{\rm CC} \to (c_{14}^2 + r_x s_{14}^2) V_{\rm CC}$;

(III) If both $\theta_{13} \neq 0$ and $\theta_{14} \neq 0$ (and $\theta_{24} = \theta_{34} = 0$), $\alpha = -s_{14} c_{13}$, $\beta = 0$, $\gamma = c_{13} c_{14}$, with the position-dependent rescaling of the standard potential $V_{\rm CC} \to (c_{14}^2 + r_x s_{14}^2) c_{13}^2 V_{\rm CC}$;

(IV) In the case of no admixture of the electron neutrino with the far states ν_3 and ν_4 ($\theta_{13} = \theta_{14} = 0$), one has $\alpha = 0$, $\beta = -s_{24}$, and $\gamma = 1$, with the position-dependent rescaling of the standard MSW potential $V_{\rm CC} \to (1 - r_x s_{24}^2) V_{\rm CC}$, in agreement with the result found in [35] for this particular case.[8]

[8] In the different parameterization adopted in [35] for the lepton mixing matrix, the role of s_{24}^2 is taken by $c_{23}^2 c_{24}^2$. In both parameterizations, the rescaling factor has (obviously) the same physical interpretation, being determined in both cases by the sterile content of the (ν_1, ν_2) sector.

In the general case the modifications are less obvious than a simple rescaling of the standard potential, as the 2×2 Hamiltonian in Eq. (A6) can contain both new diagonal and off-diagonal terms. The matrix $\bar{H}_{2\nu}$ in Eq. (A4) will be diagonalized by a 2×2 rotation

$$R_{12}^{m2\times 2}(x) = \begin{pmatrix} \cos\theta_{12}^m & \sin\theta_{12}^m \\ -\sin\theta_{12}^m & \cos\theta_{12}^m \end{pmatrix}, \tag{A14}$$

which defines the mixing angle in matter θ_{12}^m that, in general, will depend on all the mixing angles except for θ_{23}. Therefore, if we define the 4×4 rotation in the (1, 2) plane

$$R_{12}^m(x) = \begin{pmatrix} R_{12}^{m2\times 2} & 0 \\ 0 & I^{2\times 2} \end{pmatrix}, \tag{A15}$$

the starting four-dimensional Hamiltonian in Eq. (20) will be diagonalized by the matrix

$$U^m = AR_{12}^m, \tag{A16}$$

which connects the flavor eigenstates to the instantaneous energy eigenstates in matter

$$\begin{pmatrix} \nu_e \\ \nu_\mu \\ \nu_\tau \\ \nu_s \end{pmatrix} = U^m \begin{pmatrix} \nu_1^m \\ \nu_2^m \\ \nu_3^m \\ \nu_4^m \end{pmatrix}. \tag{A17}$$

The mixing angle in matter θ_{12}^m is given by

$$\frac{k_m}{k} \sin 2\theta_{12}^m = \sin 2\theta_{12} + 2 v_x r_x \alpha\beta, \tag{A18}$$

$$\frac{k_m}{k} \cos 2\theta_{12}^m = \cos 2\theta_{12} - v_x \gamma^2 - v_x r_x(\alpha^2 - \beta^2), \tag{A19}$$

where $k \equiv k_{\rm sol}$ and the neutrino wave number in matter k_m is defined by

$$\frac{k_m^2}{k^2} = [\cos 2\theta_{12} - v_x\gamma^2 - v_x r_x(\alpha^2 - \beta^2)]^2 + [\sin 2\theta_{12} + 2 v_x r_x \alpha\beta]^2, \tag{A20}$$

with $v_x = V_{\rm CC}(x)/k$. It should be noted that for $\alpha\beta < 0$ *both* terms in Eq. (A20) may become *simultaneously* small, even for large values of θ_{12}. In particular, if at a point x along the neutrino trajectory the *two* conditions[9]

$$\frac{1}{v_x^2} = [\gamma^2 + r_x(\alpha^2 - \beta^2)]^2 + 4r_x^2\alpha^2\beta^2, \tag{A21}$$

$$\tan 2\theta_{12} = \frac{2r_x|\alpha\beta|}{\gamma^2 + r_x(\alpha^2 - \beta^2)} \tag{A22}$$

are both satisfied, the difference between the two energy eigenstates in matter approaches zero ($k_m \to 0$). In such a case one expects important nonadiabatic effects encoded by a nonzero swapping probability $P_c \equiv P(\nu_2^m \to \nu_1^m)$ between the two energy eigenstates in matter. However, it turns out that the second condition [Eq. (A22)] cannot be realized for realistic values of the parameters involved in the conversion of solar neutrinos. On the one hand, the mixing angle θ_{12} is constrained to have relatively big values by the KamLAND experiment (see the left panels of Figs. 1 and 2), which sets the robust lower limit $\tan 2\theta_{12} \gtrsim 1.0$ (at the 4σ level), *independent* of any kind of matter-effects. On the other hand, the possible excursion of the right term in Eq. (A22) is severely constrained by the nonsolar neutrino oscillation phenomenology and by the properties of the Sun. Indeed we have that (I) In the Sun the ratio r_x never exceeds the maximum value (assumed at the Sun center) $r_{\max} \simeq 0.25$; (II) The mixing angles (θ_{13}, θ_{14}) are bounded by the reactor experiments ($s_{13}^2 \lesssim 0.1$ and $s_{14}^2 \lesssim 0.1$). These circumstances ensure that the numerator in the right term of Eq. (A22) is always small, while keeping its denominator close to 1. Allowing for arbitrary values of the other two mixing angles (θ_{24}, θ_{34}), we estimate that the ratio on the right side of Eq. (A22) never exceeds 0.2. Therefore, nonadiabatic effects are completely irrelevant in the problem under study, as we have explicitly checked by a numerical scan of the relevant parameter space. We stress that the same conclusion would not hold if the assumption of *CPT* invariance were abandoned, as it ensures that the mixing angles probed by the reactor antineutrinos are identical to those involved in the conversion of the solar neutrinos.

Considering an electron neutrino produced in the Sun, the probability to detect it on the Earth with flavor α will be

$$P(\nu_e \to \nu_\alpha) = \sum_{i=1}^{4} |U_{\alpha i} e^{\xi_i} U_{ei}^m|^2 \quad (\alpha = e, \mu, \tau, s), \tag{A23}$$

where the U_{ei}^m's are the mixing matrix elements calculated in the production point, while the $\xi_i \sim \Delta m_{i1}^2 L/2E$ are the phases acquired by the energy eigenstates during their propagation from the Sun center to the Earth surface ($L \simeq 1$ a.u.). The information contained in the (large) phases gets lost by the spatial average over the neutrino production zone and by the energy smearing [76], and Eq. (A23) reduces to

$$P(\nu_e \to \nu_\alpha) = \sum_{i=1}^{4} |U_{\alpha i}|^2 |U_{ei}^m|^2 \quad (\alpha = e, \mu, \tau, s), \tag{A24}$$

which coincides with the Eq. (31) used in Sec. II. In summary, the calculation of the transition probability is

[9]Equations (A21) and (A22) generalize analogous conditions introduced in [75] in the context of solar neutrino conversion in the presence of nonstandard neutrino interactions of the flavor-changing type. In that study, focused on the case of small mixing angles, it was shown that nonadiabatic effects are enhanced when: (I) $v_x = \cos 2\theta_{12} \simeq 1$ (corresponding to the common resonance condition); and (II) $\tan 2\theta_{12} = -2\epsilon_{ea}$, where the coupling constant ϵ_{ea}, parametrizing the strength of the new interaction between the two different flavors ν_e and ν_a, plays the role of our off-diagonal parameter $r_x\alpha\beta$. In the presence of additional flavor-diagonal interaction terms of the type ϵ_{ee} and ϵ_{aa} one would have the more general conditions: (I) $[1/v_x^2 = [(1 + \epsilon_{ee} - \epsilon_{aa})^2 + 4\epsilon_{ea}^2]$; and (II) $\tan 2\theta_{12} = -2\epsilon_{ea}/(1 + \epsilon_{ee} - \epsilon_{aa})$. In our case the diagonal terms correspond to $\epsilon_{ee} = -1 + \gamma^2 + r_x\alpha^2$ and $\epsilon_{aa} = r_x\beta^2$ [see Eq. (A6)].

reduced to the following steps: (I) Given the four mixing angles (θ_{13}, θ_{14}, θ_{24}, θ_{34}), as defined in the parameterization in Eq. (1), calculate the coefficients (α, β, γ) making use of Eqs. (A7)–(A9); (II) Determine how the mixing angle θ_{12} in vacuum gets modified in matter applying Eqs. (A18)–(A20) for the expression of θ_{12}^m; (III) Deduce the electron neutrino mixing elements U_{ei}^m in matter from Eq. (A16); (IV) Derive the transition probabilities $P(\nu_e \to \nu_\alpha)$ using Eq. (A24).

APPENDIX B: GENERALIZATION TO A 3 + s SCHEME

The generalization to more than one sterile specie is straightforward and is obtained by observing that the 2×2 matrix $\bar{H}_{2\nu}^{\rm dyn}$ entailing the nontrivial dynamics is always given by the submatrix with indices (1, 2) of the matrix

$$\bar{H}^{\rm dyn} = A^T V A, \tag{B1}$$

where now A, still defined as $A = UR_{12}^T$ like in the 3 + 1 scheme, has dimension $3+s$, and the matrix V is given by $\mathrm{diag}(V_{\rm CC}, 0, 0, -V_{\rm NC}, -V_{\rm NC}, \ldots)$. If the matrix A is taken with the product $R_{1,3+s}\ldots R_{14}R_{13}$ of the matrices involving the first index as its rightmost factor (ensuring $A_{12}=0$), the effective 2×2 Hamiltonian $\bar{H}_{2\nu}^{\rm dyn}$ has the same form of Eq. (A6) provided that the (combinations of the) three coefficients (α, β, γ) appearing in Eq. (A6) are replaced as follows:

$$\alpha^2 \to \sum_{i=1}^{s}\alpha_i^2, \tag{B2}$$

$$\beta^2 \to \sum_{i=1}^{s}\beta_i^2, \tag{B3}$$

$$\alpha\beta \to \sum_{i=1}^{s}\alpha_i\beta_i, \tag{B4}$$

with

$$\alpha_i = A_{3+i,1} \qquad (i=1,\ldots,s), \tag{B5}$$

$$\beta_i = A_{3+i,2} \qquad (i=1,\ldots,s), \tag{B6}$$

while

$$\gamma^2 \to 1 - U_{e3}^2 - \sum_{i=4}^{3+s}U_{ei}^2. \tag{B7}$$

From this last formula it is evident that the role of the electron neutrino mixing with additional sterile species is completely symmetrical to that played by the fourth one.

APPENDIX C: INCLUSION OF EARTH MATTER EFFECTS

We briefly review the analytical results pertaining Earth matter effects, for the sake of completeness and self-consistency of the paper. In general, Earth matter effects, intervening prior to the detection of the solar neutrinos, can be implemented by the following substitution in Eq. (31):

$$U_{\alpha i}^2 \to P_{\alpha i} \qquad (i = 1,2,3,4;\ \alpha = e,\mu,\tau,s), \tag{C1}$$

where $P_{\alpha i} \equiv P(\nu_i \to \nu_\alpha)$ are the conversion probabilities in the Earth of the mass eigenstates into the flavor ones. Although the $P_{\alpha i}$'s can be calculated numerically, it is possible to simplify their evaluation by reducing the 4ν dynamics to that of a 2ν system, in analogy with the solar-matter induced effects discussed in Appendix A. In fact, the $P_{\alpha i}$'s, can always be written as

$$P_{\alpha i} = |(AWR_{12})_{\alpha i}|^2 \equiv |(AZ_{12})_{\alpha i}|^2, \tag{C2}$$

where, from right to left: (I) The matrix R_{12} rotates the initial mass eigenstates into the auxiliary flavor basis $\bar{\nu}$ defined in Eq. (A1); (II) The matrix W contains the (complex) transition amplitudes among the eigenstates of such new basis, whose nontrivial dynamics is confined to the ($\bar{\nu}_1$, $\bar{\nu}_2$) sector; (III) Finally, the matrix A rotates back the auxiliary basis $\bar{\nu}$ to the standard flavor basis. The 4×4 matrix W contains in its (1, 2) sub-block the nontrivial information as follows:

$$Z_{12} = WR_{12} = \begin{pmatrix} \sqrt{P}e^{-i\xi} & \sqrt{1-P}e^{-i\eta} & 0 & 0 \\ -\sqrt{1-P}e^{i\eta} & \sqrt{P}e^{i\xi} & 0 & 0 \\ 0 & 0 & 1 & 0 \\ 0 & 0 & 0 & 1 \end{pmatrix}, \tag{C3}$$

where the 2-flavor transition probability $P \equiv \bar{P}_{e1}^{2\nu} = 1 - \bar{P}_{e2}^{2\nu}$ and the two phases (ξ, η) must be calculated numerically by implementing the MSW Hamiltonian of the form given in Eq. (A6), with number densities $N_e(x)$ and $N_n(x)$ evaluated along the neutrino trajectory in the Earth interior. From Eq. (C2) one obtains for the transition probabilities into electron neutrinos

$$P_{e1} = |A_{11}Z_{11} + A_{12}Z_{21}|^2, \tag{C4}$$

$$P_{e2} = |A_{11}Z_{12} + A_{12}Z_{22}|^2, \tag{C5}$$

$$P_{e3} = A_{13}^2 \equiv U_{e3}^2, \tag{C6}$$

$$P_{e4} = A_{14}^2 \equiv U_{e4}^2, \tag{C7}$$

which, taking into account the expressions of the elements of the first row of the matrix A $(A_{11}, A_{12}, A_{13}, A_{14} = c_{14}c_{13}, 0, c_{14}s_{13}, s_{14})$, become

$$P_{e1} = c_{14}^2 c_{13}^2 \bar{P}_{e1}^{2\nu}, \tag{C8}$$

$$P_{e2} = c_{14}^2 c_{13}^2 \bar{P}_{e2}^{2\nu}, \tag{C9}$$

$$P_{e3} = c_{14}^2 s_{13}^2, \tag{C10}$$

$$P_{e4} = s_{14}^2, \tag{C11}$$

which constitute the generalization of the 3-flavor expressions used in the literature. It should be noted that in our parameterization it is $A_{12} = 0$, and we can express the 4ν transition probabilities in terms of the 2-flavor transition *probability* $\bar{P}_{1e}^{2\nu}$, the knowledge of the phases (ξ, η) being unnecessary. For the transition probabilities into sterile neutrinos, one obtains the analogous expressions

$$P_{s1} = |A_{41}Z_{11} + A_{42}Z_{21}|^2, \tag{C12}$$

$$P_{s2} = |A_{41}Z_{12} + A_{42}Z_{22}|^2, \tag{C13}$$

$$P_{s3} = A_{43}^2 \equiv U_{s3}^2, \tag{C14}$$

$$P_{s4} = A_{44}^2 \equiv U_{s4}^2, \tag{C15}$$

which, in the limit of no matter effects ($Z_{12} = R_{12}$), return the expressions of U_{si}^2 given in Eqs. (11)–(14). Now, differently form the case of the electron neutrinos, both elements A_{41} and A_{42} can be different from zero [see Eqs. (15)–(18)], and one cannot express the 4-flavor transition probabilities P_{s1} and P_{s2} in terms of the 2-flavor transition *probability* $\bar{P}_{1e}^{2\nu}$, needing the complete information on the (complex) 2-flavor transition *amplitudes*, having phases (ξ, η). We close this Appendix by stressing that the expressions given in Eqs. (C4), (C7), (C12), and (C15) are valid for any parameterization of the mixing matrix of the form $U = AR_{12}$. The validity of Eqs. (C8) and (C11) is instead restricted to the case in which the matrix A is of the form $A = BR_{14}R_{13}$.

APPENDIX D: POTENTIAL SENSITIVITY TO THE *CP* VIOLATING PHASES

For definiteness, in the rest of the paper we have restricted ourselves to the case of vanishing *CP* violating phases. Here, we briefly comment on the potential sensitivity of solar neutrinos to them. In the 3-flavor framework one can always eliminate the *CP* violating phase δ appearing in the mixing matrix from all the observable quantities involved in the solar neutrino transitions [77,78], since the two following conditions hold: (I) All the relevant information on the flavor conversion is contained in the survival probability P_{ee} of the electron neutrinos, as one cannot distinguish ν_μ from ν_τ at low energies and by unitarity it is $P_{e\mu} + P_{e\tau} = 1 - P_{ee}$; (II) The phase δ can be eliminated from the expression of P_{ee} since it can be rotated away from the MSW dynamics due to the particular form of the potential [77,78] (see also [79,80]).

The same conclusion is not true in the 4-flavor case since the two conditions above are no more valid, as we briefly show. Without loss of generality we can assign one of the three phases to the (2, 3) sector since, as we have seen in Sec. II and Appendix A, the associated mixing angle θ_{23} can be eliminated from the description of the solar neutrino conversion. We can then attribute the remaining two phases to the (1, 3) and (1, 4) sectors by defining the complex mixing matrix as

$$U = \tilde{R}_{23}R_{24}R_{34}\tilde{R}_{14}\tilde{R}_{13}R_{12}, \tag{D1}$$

where $\tilde{R}_{ij}$ is a 4×4 complex rotation in the (i, j) plane, formed by replacing the real 2×2 submatrix in Eq. (2) with the complex one

$$\tilde{R}_{ij}^{2\times2} = \begin{pmatrix} \tilde{c}_{ij} & \tilde{s}_{ij}^* \\ -\tilde{s}_{ij} & \tilde{c}_{ij} \end{pmatrix}, \tag{D2}$$

with $\tilde{c}_{ij} \equiv \cos\theta_{ij}$, $\tilde{s}_{ij} \equiv \sin\theta_{ij}e^{i\delta_{ij}}$. The two phases δ_{13}, δ_{14} will appear in the expression of the transition probability P_{es} in Eq. (A23) through the (now complex) elements U_{si} [see Eqs. (11)–(14)]. Furthermore, they will enter at the dynamical level by affecting both P_{ee} and P_{es} through the expressions of the mixing elements U_{ei}^m in matter, which are determined by the diagonalization of the Hamiltonian

$$\bar{H}_{2\nu}^{\text{dyn}} = V_{\text{CC}}(x)\begin{pmatrix} \gamma^2 + r_x|\alpha|^2 & r_x\alpha^*\beta \\ r_x\alpha\beta^* & r_x|\beta|^2 \end{pmatrix}, \tag{D3}$$

where the two parameters α and β can be complex numbers. With our choice of the phases, $\beta = -s_{24}$ is still real, while α is complex and is obtained with the replacements $(s_{13} \to \tilde{s}_{13}, s_{14} \to \tilde{s}_{14})$ in its expression in Eq. (A7).

We postpone to a future work the study of the complex extension of the treatment we have provided for the real case. Here we just limit ourselves to observe that the *CP* phases always appear in terms involving two small mixing angles, and therefore it is difficult to observe their effects in current solar neutrino experiments. Finally, we stress that for $\theta_{24} = \theta_{34} = 0$ the *CP* phases disappear from the description of the solar neutrino transitions, thus rendering the numerical results presented in Sec. III independent of them.

[1] T. A. Mueller *et al.*, Phys. Rev. C **83**, 054615 (2011).
[2] P. Vogel, G. K. Schenter, F. M. Mann, and R. E. Schenter, Phys. Rev. C **24**, 1543 (1981).
[3] F. Von Feilitzsch, A. A. Hahn, and K. Schreckenbach, Phys. Lett. B **118**, 162 (1982).
[4] K. Schreckenbach, G. Colvin, W. Gelletly, and F. Von Feilitzsch, Phys. Lett. B **160**, 325 (1985).
[5] A. A. Hahn, K. Schreckenbach, G. Colvin, B. Krusche, W. Gelletly, and F. Von Feilitzsch, Phys. Lett. B **218**, 365 (1989).
[6] G. Mention *et al.*, Phys. Rev. D **83**, 073006 (2011).
[7] J. N. Abdurashitov *et al.*, Phys. Rev. C **73**, 045805 (2006).
[8] C. Giunti and M. Laveder, arXiv:1006.3244.
[9] A. Aguilar *et al.* (LSND Collaboration), Phys. Rev. D **64**, 112007 (2001).
[10] A. A. Aguilar-Arevalo *et al.* (MiniBooNE Collaboration), Phys. Rev. Lett. **98**, 231801 (2007).
[11] A. A. Aguilar-Arevalo *et al.* (MiniBooNE Collaboration), Phys. Rev. Lett. **103**, 111801 (2009).
[12] J. Kopp, M. Maltoni, and T. Schwetz, arXiv:1103.4570.
[13] C. Giunti and M. Laveder, Phys. Rev. D **83**, 053006 (2011).
[14] J. Hamann, S. Hannestad, G. G. Raffelt, I. Tamborra, and Y. Y. Y. Wong, Phys. Rev. Lett. **105**, 181301 (2010).
[15] E. Giusarma *et al.*, arXiv:1102.4774 [Phys. Rev. D (to be published)].
[16] S. Hannestad, Phys. Rev. Lett. **95**, 221301 (2005).
[17] J. R. Kristiansen and O. Elgaroy, arXiv:1104.0704 [Astron. Astrophys. (to be published)].
[18] Y. I. Izotov and T. X. Thuan, Astrophys. J. **710**, L67 (2010).
[19] G. Mangano and P. D. Serpico, arXiv:1103.1261.
[20] P. C. de Holanda and A. Yu. Smirnov, Phys. Rev. D **69**, 113002 (2004).
[21] P. C. de Holanda and A. Yu. Smirnov, arXiv:1012.5627 [Phys. Rev. D (to be published)].
[22] R. Abbasi *et al.* (IceCube Collaboration), Phys. Rev. D **83**, 012001 (2011).
[23] H. Nunokawa, O. L. G. Peres, and R. Zukanovich Funchal, Phys. Lett. B **562**, 279 (2003).
[24] S. Choubey, J. High Energy Phys. 12 (2007) 014.
[25] S. Razzaque and A. Yu. Smirnov, arXiv:1104.1390.
[26] V. D. Barger, N. Deshpande, P. B. Pal, R. J. N. Phillips, and K. Whisnant, Phys. Rev. D **43**, R1759 (1991).
[27] P. I. Krastev, S. T. Petcov, and L. Qiuyu, Phys. Rev. D **54**, 7057 (1996).
[28] C. Giunti, M. C. Gonzalez-Garcia, and C. Pena-Garay, Phys. Rev. D **62**, 013005 (2000).
[29] J. N. Bahcall, M. C. Gonzalez-Garcia, and C. Pena-Garay, Phys. Rev. C **66**, 035802 (2002).
[30] P. C. de Holanda and A. Yu. Smirnov, arXiv:hep-ph/0211264.
[31] J. N. Bahcall, M. C. Gonzalez-Garcia, and C. Pena-Garay, J. High Energy Phys. 02 (2003) 009.
[32] M. Maltoni, T. Schwetz, M. A. Tortola, and J. W. F. Valle, Phys. Rev. D **67**, 013011 (2003).
[33] M. Cirelli, G. Marandella, A. Strumia, and F. Vissani, Nucl. Phys. B **708**, 215 (2005).
[34] M. C. Gonzalez-Garcia and M. Maltoni, Phys. Rep. **460**, 1 (2008).
[35] D. Dooling, C. Giunti, K. Kang, and C. W. Kim, Phys. Rev. D **61**, 073011 (2000).
[36] M. Apollonio *et al.* (CHOOZ Collaboration), Eur. Phys. J. C **27**, 331 (2003).
[37] Y. Declais *et al.*, Nucl. Phys. B **434**, 503 (1995).
[38] G. L. Fogli, E. Lisi, A. Marrone, A. Palazzo, and A. M. Rotunno, Phys. Rev. Lett. **101**, 141801 (2008).
[39] A. Palazzo, Phys. Rev. D **83**, 101701(R) (2011).
[40] A. Palazzo and J. W. F. Valle, Phys. Rev. D **80**, 091301(R) (2009).
[41] C. Giunti and Y. F. Li, Phys. Rev. D **80**, 113007 (2009).
[42] J. Schechter and J. W. F. Valle, Phys. Rev. D **22**, 2227 (1980).
[43] K. Nakamura *et al.* (Particle Data Group), J. Phys. G **37**, 075021 (2010).
[44] M. Maltoni and T. Schwetz, Phys. Rev. D **76**, 093005 (2007).
[45] P. Adamson *et al.* (The MINOS Collaboration), Phys. Rev. D **81**, 052004 (2010).
[46] L. Wolfenstein, Phys. Rev. D **17**, 2369 (1978).
[47] S. P. Mikheev and A. Yu. Smirnov, Yad. Fiz. **42**, 1441 (1985) [Sov. J. Nucl. Phys. **42**, 913 (1985)].
[48] T. K. Kuo and J. T. Pantaleone, Rev. Mod. Phys. **61**, 937 (1989).
[49] X. Shi and D. N. Schramm, Phys. Lett. B **283**, 305 (1992).
[50] G. L. Fogli, E. Lisi, and D. Montanino, Phys. Rev. D **49**, 3626 (1994).
[51] G. L. Fogli, E. Lisi, A. Marrone, and A. Palazzo, Prog. Part. Nucl. Phys. **57**, 742 (2006).
[52] B. T. Cleveland *et al.*, Astrophys. J. **496**, 505 (1998).
[53] J. N. Abdurashitov *et al.* (SAGE Collaboration), J. Exp. Theor. Phys. **95**, 181 (2002).
[54] W. Hampel *et al.* (GALLEX Collaboration), Phys. Lett. B **447**, 127 (1999).
[55] M. Altmann *et al.* (GNO Collaboration), Phys. Lett. B **616**, 174 (2005).
[56] T. Kirsten, J. Phys. Conf. Ser. **120**, 052013 (2008).
[57] S. Fukuda *et al.* (Super-Kamiokande Collaboration), Phys. Rev. Lett. **86**, 5651 (2001); **86**, 5656 (2001); Phys. Lett. B **539**, 179 (2002).
[58] Q. R. Ahmad *et al.* (SNO Collaboration), Phys. Rev. Lett. **87**, 071301 (2001); **89**, 011301 (2002); **89**, 011302 (2002).
[59] S. N. Ahmed *et al.* (SNO Collaboration), Phys. Rev. Lett. **92**, 181301 (2004).
[60] B. Aharmim *et al.* (SNO Collaboration), Phys. Rev. C **72**, 055502 (2005).
[61] B. Aharmim *et al.* (SNO Collaboration), Phys. Rev. Lett. **101**, 111301 (2008).
[62] G. Bellini *et al.* (Borexino Collaboration), arXiv:1104.1816.
[63] G. Bellini *et al.* (Borexino Collaboration), Phys. Rev. D **82**, 033006 (2010).
[64] B. Aharmim *et al.* (SNO Collaboration), Phys. Rev. C **81**, 055504 (2010).
[65] A. Gando *et al.* (KamLAND Collaboration), Phys. Rev. D **83**, 052002 (2011).
[66] A. B. Balantekin and D. Yilmaz, J. Phys. G **35**, 075007 (2008).
[67] T. Schwetz, M. Tortola, and J. W. F. Valle, New J. Phys. **10**, 113011 (2008).

[68] H. L. Ge, C. Giunti, and Q. Y. Liu, Phys. Rev. D **80**, 053009 (2009).
[69] M. C. Gonzalez-Garcia, M. Maltoni, and J. Salvado, J. High Energy Phys. 04 (2010) 056.
[70] T. Schwetz, M. Tortola, and J. W. F. Valle, arXiv:1103.0734.
[71] F. L. Villante, G. Fiorentini, and E. Lisi, Phys. Rev. D **59**, 013006 (1998).
[72] G. L. Fogli, E. Lisi, A. Palazzo, and F. L. Villante, Phys. Rev. D **63**, 113016 (2001).
[73] S. Goswami and A. Yu. Smirnov, Phys. Rev. D **72**, 053011 (2005).
[74] G. L. Fogli, E. Lisi, A. Marrone, and A. Palazzo, *Proceedings of the International Workshop: Neutrino Oscillations*, edited by M. Baldo Ceolin (University of Padova, Padova, Italy, 2006), Vol. 1, p. 69.
[75] S. Bergmann, Nucl. Phys. B **515**, 363 (1998).
[76] E. Lisi, A. Marrone, D. Montanino, A. Palazzo, and S. T. Petcov, Phys. Rev. D **63**, 093002 (2001).
[77] T. K. Kuo and J. T. Pantaleone, Phys. Lett. B **198**, 406 (1987).
[78] H. Minakata and S. Watanabe, Phys. Lett. B **468**, 256 (1999).
[79] H. Yokomakura, K. Kimura, and A. Takamura, Phys. Lett. B **544**, 286 (2002).
[80] A. B. Balantekin, J. Gava, and C. Volpe, Phys. Lett. B **662**, 396 (2008).